DOI 10.7343/as-2023-608

ACQUE SOTTERRANEE
Italian Journal of Groundwater

2023-AS44-608: 39- 51

journal homepage: https://www.acquesotterranee.net/

Hydrogeological characterization of the Complex Terminal aquifer using geoelectrical investigation in the arid environment of Chetma-Biskra (South-East of Algeria)

Caratterizzazione idrogeologica tramite prospezione geoelettrica dell'acquifero "Complex Terminal" nell'ambiente arido di Chetma-Biskra (sud-est dell'Algeria)

Farès Kessasra[a,b,c], **Nour El Houda Mezerreg**[e], **Djamel Eddine Dehibi**[b], **Lamine Djaret**[b], **Asma Bouhchicha**[d], **Mohamed Mesbah**[c]

[a] Geological Engineering Laboratory (LGG), Geology team 3, University of Jijel, Campus central, BP 98, 18 000 Jijel, Algeria
[b] Département des Sciences de la Terre et de l'Univers, University of Jijel, BP 98, 18 000 Jijel, Algeria
email : *f.kessasra@univ-jijel.dz, fareskessasra@yahoo.fr*
[c] Département de Géologie, Faculté des Sciences de la Terre, de Géographie et d'Aménagement du Territoire, Université des Sciences et de la Technologie Houari Boumediène. BP 32 El Alia, Algiers, Algeria
[d] Entreprise Nationale de Géophysique, ENAGEO, BP 140, Hassi Messaoud, Ouargla, Algeria
[e] Département des sciences géologiques, Université de Constantine 1, 25 000 Algeria

ARTICLE INFO

Ricevuto/*Received*: 3 January 2023
Accettato/*Accepted*: 23 March 2023
Pubblicato online/*Published online*: 30 March 2023

Handling Editor:
Marco Rotiroti

Citation:
Kessasra, F., Mezerreg, NEH., Dehibi, DE., Djaret, L., Bouhchicha, A., Mesbah, M. (2023). Hydrogeological characterization of the Complex Terminal aquifer using geoelectrical investigation in the arid environment of Chetma-Biskra (South-East of Algeria) Acque Sotterranee - *Italian Journal of Groundwater*, 12(1), 39 - 51
https://doi.org/10.7343/as-2023-608

Correspondence to:
Farès Kessasra
f.kessasra@univ-jijel.dz
fareskessasra@yahoo.fr

Keywords: *geoelectrical investigation, groundwater, Complex Terminal Aquifer, Droh Anticline, Biskra, Algeria.*

Parole chiave: indagine geoelettrica, acque sotterranee, Acquifero Complex Terminal, anticlinale Droh, Biskra, Algeria .

Riassunto

Come area idrogeologica di transizione, Biskra (Algeria) detiene grandi risorse di acque sotterranee in acquiferi profondi, come quello denominato Complex Terminal. A causa della crescente domanda di acqua per fini potabili ed irrigui, e di un basso tasso di ricarica, questa regione arida sta affrontando una grande carenza di acqua. Emerge quindi la necessità di promuovere prospezioni idrogeologiche. Nel presente lavoro svolto sull'area di Chetma è stato adottato un approccio integrato, comprendente indagini geofisiche corredate dall'analisi del contesto geologico e idrogeologico. I risultati evidenziano la presenza di una struttura profonda con caratteristiche idrogeologiche rilevanti. Sono stati infatti identificati due corpi resistivi, composti da calcari con pieghe anticlinali, chiamati Droh, che ospitano un alto piezometrico, e un corpo deposizionale conduttivo con pieghe sinclinali. La formazione del Maastrichtiano è sede di un acquifero complesso costituito da calcari fratturati, spessi circa 200-350 m, e da calcari e calcari marnosi dell'Eocene inferiore. Oltre i 400 m di profondità, i pozzi che captano i calcari della formazione Maastrichtiana hanno un grande rendimento, con portate tra 25 e 90 L/s. Alla profondità di circa 300 m, le portate si attestano in media intorno a 40 L/s. Al contrario, le formazioni con pieghe sinformi caratterizzate da un alto contenuto di argille e marne restituiscono un basso rendimento idraulico. Questo studio conferma la presenza di acquiferi fratturati potenzialmente sfruttabili e fornisce nuove informazioni per migliorare la captazione delle acque sotterranee, in modo da soddisfare l'aumento del fabbisogno idrico domestico e irriguo atteso per il 2030.

Abstract

As a transition hydrogeological area, Biskra (Algeria) holds large groundwater resources in deeply buried aquifers such as the Complex Terminal. Due to a growing demand of drinking water supply and irrigation combined to low recharge, this arid region is facing an acute shortage of water and hence, the need for groundwater investigation. We used an integrated approach including geophysical investigation correlated to the geological and hydrogeological context in the Chetma area. The results highlight a deep structural form with significant hydrogeological features. In fact, two resistant limestone anticlines called Droh corresponding to a piezometric dome and a syncline filled with conductive deposit materials were identified. The Maastrichtian formation, consisting of fractured limestone, about 200 to 350 m thick, together with Lower Eocene marl limestone and limestone form a complex aquifer. At more than 400 m depth, boreholes capturing Maastrichtian limestone offer a high yield ranging from 25 to 90 L/s. Moreover, groundwater yield provides an average of 40 L/s at 300 m of depth. In contrast, synform geometries with high clay and marl content offer a weak groundwater yield. We confirmed the occurence of fractured aquifers which could constitute potentially groundwater production zones. This study provides new insights to enhance groundwater pumping for domestic and irrigation purposes for 2030.

Introduction

Groundwater is considered the largest resource of fresh water at global scale and plays a vital role in securing the water supply and irrigation in arid environments when surface water resources are limited (Azffri et al., 2022). Due to the expansion of water use, overexploitation and pollution, groundwater availability decreased (Albrecht et al., 2017) and declined in quality. Constituting a reliable source of water for irrigation in the Middle East and North Africa (Molle & Closas, 2017; Wada et al., 2010), groundwater is embedded in irrigation scheme. More than 50% of the total irrigation water demand in MENA is satisfied through groundwater (Wada et al., 2010). Unconfined aquifers provide the only permanent freshwater resource for most of the population in MENA (Boucher et al., 2009). Agricultural water withdrawals are approximated to be about 70% of all water withdrawn with up to 90% share in arid countries (Bogardi et al., 2021).

In this context, the use of geophysical methods are useful for groundwater investigation. Electrical and seismic prospecting methods have confirmed their high efficiency and performance (Goldman and Neubauer, 1994; Choudhury et al., 2004; Boucher et al., 2009; Bersi et al., 2020; Ben Alayet et al., 2021). Geophysical prospecting using direct electric current injection is an appropriate tool for investigating deep formations. Several intrinsic factors such as depth of the aquifer and geological features impact the groundwater investigation. Resistivity profiling is often correlated with lithological logs and mechanical soundings to determine the thickness and resistivity of different layers and achieve the hydrogeological characterization. Nevertheless, serious uncertainties could emerge in the case of formations with similar resistivities (Choudhury et al., 2004)

The Algerian Sahara contains deeply buried aquifers and their hydrogeological features require the application of high-yield investigation methods. A vital resource in an arid region, the Continental Intercalar and Complex Terminal aquifers are a unique perennial resource (Guendouz et al., 2006). Due to the overexploitation related to the increased water demand for drinking supply and irrigated areas and the decrease in recharge, groundwater depletion and salinity increase were observed in Biskra.

In fact, estimated at 775,797 inhabitants in 2010, population in Biskra would reach 1,039,953 inhabitants in 2030 (Tab. 1). Indeed, drinking water demand was established at 63.6 hm^3/year for all the province, in which Biskra and Chetma represent 24.52 hm^3/year deserving 227,620 inhabitants (35% of the total demand). In 2030 Biskra and Chetma would reach 338,112 inhabitants generating a water demand of 35.14 hm^3/year on a total demand of 93 hm^3/year for all the province (PNE, 2010). The available sources of water supply in Biskra are limited to groundwater. Water supply is insured through boreholes and springs located at Chetma and Droh fields. Water authorities investigate the best way to enhance pumping capacity by 2030.

The main objectives of this study are (i) to achieve an integrated approach including socioeconomic, geological and hydrogeological context and geophysical investigations which resolves the lithological and hydrogeological uncertainties, (ii) to investigate the local Complex Terminal aquifer using Vertical Electrical Soundings (VES), iso-apparent resistivity maps, and geoelectrical sections in order to better understand and evaluate the local groundwater capacity, and finally (iii) to assess a correlation between geophysical issues and aquifer characteristics by identifying the most suitable drilling locations. This study gives new insights to enhance groundwater pumping by 2030 in response to the predictions of the National Water Plan (PNE, 2010).

Material and methods

Site description

Biskra is divided into four geomorphological groups with a mountainous area bordering the North, plateaus in the West; plains in the East, depressions and Chotts in the South-East and Saharan plain in the South (Fig. 1). Located in an arid zone, the area is characterized by low precipitation (150 mm/year) and high temperature (an average of 20.9°C). Biskra is part of Chott Melrhir basin which is drained by Oued (Wadi) Djedi, Oued Biskra, and Oued Abdi. Due to the high evaporation, infiltration, and withdrawals, the watercourses dried. Except for Oued El Abiod, which remains perennial up to the piedmont, whose Foum El Gherza dam provides irrigation water (Aidaoui, 1994; Remini, 2018).

The utilized agricultural area is estimated at 174,132 ha which includes an irrigated area of 84,285 ha (PNE, 2010). A large irrigation perimeter exists at El Outaya extending on 950 ha and irrigated from the Fontaine des Gazelles dam. Two main agricultural areas exist, West Ziban and East Ziban (Tab. 2). Comparing the utilized agricultural area, West Ziban, established at 38,347 ha, appears greater about 45.5% of the total area. Cereal occupy a large part in East Ziban. Gravity irrigation is the most used method with 83.9%, drop-by-drop remains under developed. 78,982 ha are irrigated from Mio-Pliocene and Maastrichtian aquifers and only 5,303 ha irrigated from surface water. Small and medium hydraulic demand was evaluated at 1,400 hm^3 representing 40% more than the groundwater pumping. Groundwater and surface water supply were estimated at 1,095 hm^3 of which 1,000 hm^3 represent groundwater supplies. Observations agree with the overexploitation of the local aquifers (PNE, 2010).

Geology

Previous geological studies have been completed (Laffitte, 1939; Gouskov, 1964; Busson, 1970; Guiraud, 1970; ERESS, 1972; Chabbah, 2007). Considered as a transition area between mountainous Atlasic domains in the North and Saharan lands in the South which are separated by the South Atlas accident named Saharan flexure (Fig. 1). This study is focused on the Biskra-Droh Basin, a «synorogenic» region linked to the atlas orogen tectonics. The region belongs to a set of independent diachronic sedimentary areas superimposed on the Tellian Hercynian orogeny (Guiraud,

Tab. 1 - Real and projected agglomerated population and drinking water demands from 2010 to 2030 in Biskra and Chetma cities (PNE 2010).

Tab. 1 - Popolazione aggregata reale e prevista e domanda di acqua potabile dal 2010 al 2030 nelle città di Biskra and Chetma (PNE 2010).

	Agglomerated population (inhabitants)		Drinking water supply needs (hm^3/year)		Drinking water supply demand (hm^3/year)	
	Province of Biskra	Biskra and Chetma cities	Province of Biskra	Biskra and Chetma cities	Province of Biskra	Biskra and Chetma cities
2010	660,519	227,620	31,1	12.13	63,6	24.52
2015	761,990	258,268	36,9	13.75	65,0	22.00
2020	856,890	285,847	44,1	16.10	67,4	22.54
2025	950,215	313,174	53,4	19.55	76,4	25.75
2030	1,039,953	338,112	68,0	26.79	92,9	35.14

Tab. 2 - Technical characteristic comparison between Ziban West Area and Ziban East Area (PNE 2010).

Tab. 2 - Confronto delle caratteristiche tecniche tra l'area occidentale e quella orientale di Ziban (PNE 2010).

	Utilized total agricultural area		Utilized physical agricultural area		Groundwater		Surface water		Cereal		Truck farming		Irrigation method
	ha	%	ha	%	ha	%	ha	%	ha	%	ha	%	%
Ziban West area	63,887	36.68	38,347	45,49	37,801	47,86	546	10,29	5,143	19,10	5,313	30,58	Gravity irrigation 74,48
Ziban East area	81,540	46,82	36,925	43,80	34,337	43,47	2588	48,80	18,192	67,58	10,994	63,27	Gravity irrigation 92,99

1990). Large depressions fulfilled with quaternary sediments formed the central part of the basin and were separated by limited mountainous landforms or intersected by transverse accidents. First, the South-atlas Accident is a continuous line of faults and flexures that connects the monotonous Saharan domain and Atlas Mountain ranges. Indeed, the Atlas domain corresponds to two large structures: the Saharan Atlas and the Aures displaced according to a dexterous movement and connected by a hinge area in M'Doukal-Biskra. In the Northern border, the Upper Miocene is deformed in the Aures through a replay of Atlas structures and the emergence of new structures in an oblique position.

Biskra-Droh basin is dominated by Cretaceous limestone and marl with a little clay at the top and Neogene formations which consist of a heterogeneous filling of sandy and gypseous clay, sandstones and conglomerates (Fig. 2, Fig. 3). The main outcrops are located in the border. On the other hand, neogenic deposits are embedded under thick and quaternary formations that cover them in discordance and often rest in discordance on formations from Oligocene, Eocene, and Upper Cretaceous in the central part (Brinis, 2011). Chebbah established a North-South profile at Droh in 2007 (Fig. 4). The base is constituted by gypseous clays forming the Southern flank of the Droh anticline. Their thickness varies between 20 and 90 m. Two lithological groups were identified : gypseous clays and sandstone clays group and sandstone-conglomerate group deposed as transverse bars or channels strongly tectonized. In the North-East of Chetma, a fault at N120E straightens the series almost vertically. The whole is surmounted by Quaternary yellow sandy clays and rests on the Cretaceous limestone. The Droh section illustrates a straightened limestone substratum in discordance with a thick clay formation which constitutes the base of the neogenic series as shown by Droh borehole: alternation of red sandy and gypseous clays with conglomerate (0–125 m), conglomerate (125–165 m), Maastrichtian massive limestone (165–276 m) and marl with Campanian sandstone (276–340 m).

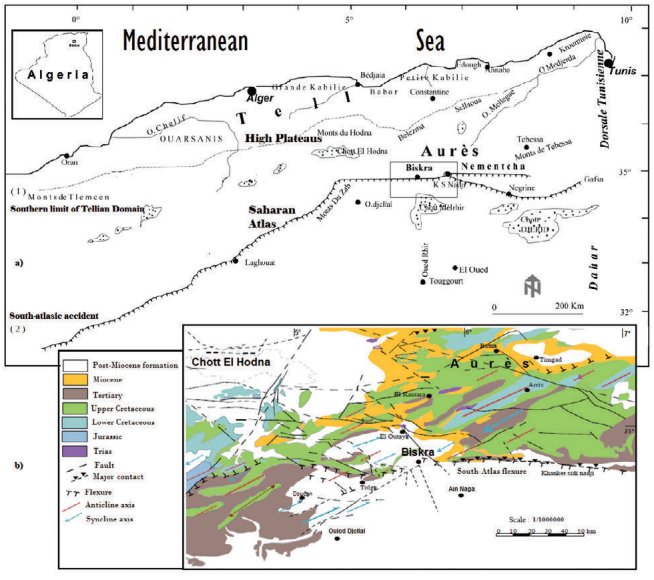

Fig. 1 - a) Location of the study area b) geological map and tectonic elements of Biskra and adjacent areas (Guiraud, 1973).

Fig. 1 - a) Ubicazione dell'area di studio b) Carta geologica ed elementi tettonici di Biskra e delle aree limitrofe (Guiraud, 1973).

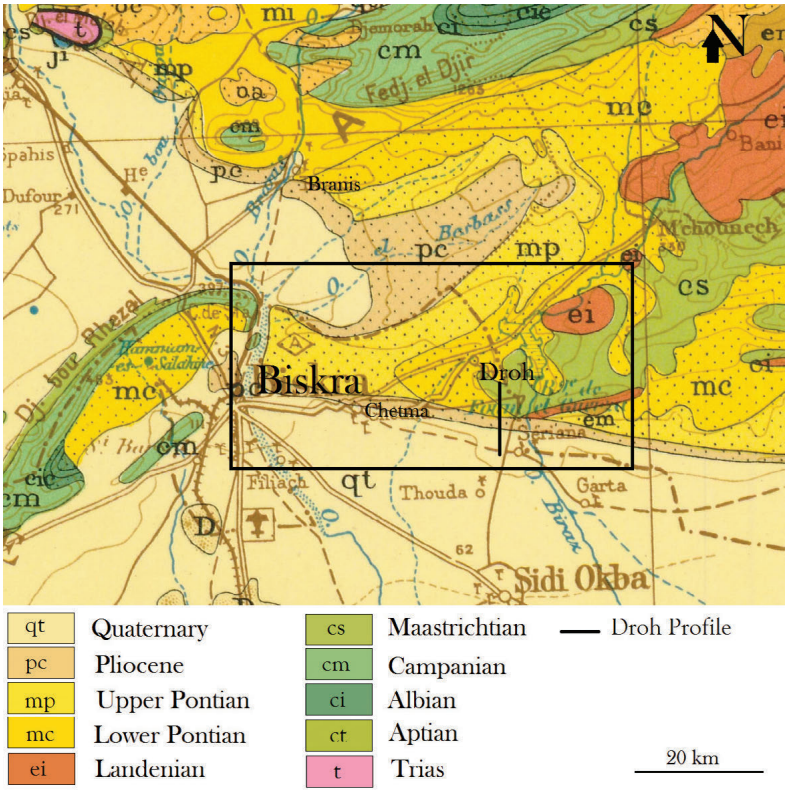

Fig. 2 -Local geological context of Biskra (Guiraud, 1973).

Fig. 2 - Assetto geologico locale di Biskra (Guiraud, 1973).

Period	Era	Stratigraphy	Lithological description
Quaternary			Clayey sands and Raw Gray Limestone
Neogene	Pliocene		Conglomerates and sandstone lees
	Late Miocene		Greenish-grey marls and gypsum intercalations
	Lower and middle Miocene		Yellow conglomerates, clays and rarely limestones and gypsums
Paleogene	Oligocene		Alternation of brown sandstone and red sandstone
	Eocene		Eocene Dolomitic limestone and rare gray clay past
	Paleocene		Marl to past limestone
Upper cretaceous	Maastrichian		Marl and limestone intercalation
	Campanian		Gray clayey marls and isolated layer of marly limestone
	Santonian		Laminated Marl and benches of limestone
	Coniacian		Alternation of clayey marls and layers of organogenesis limestones
	Turonian		Stratification of limestone and clayey marl
	Cenomanian		Marl, ammonia and limestone
Lower Cretaceous	Albian		sandstone marl formed by alternating sandstone, carbonated facies represented by limestone
	Aptian		clays and anhydrite marls
	Barremian		Red sandstone and some clayey intercalations
	Neocomian		Clay-sandstone trend and intercalations of limestone and dolomites
Trias			Clays (variegated or purple) gypsiferous and saliferous

Fig. 3 - Synthetic stratigraphy section of the study site (Guiraud, 1973).

Fig. 3 - Sezione stratigrafica esemplificativa dell'area di studio (Guiraud, 1973).

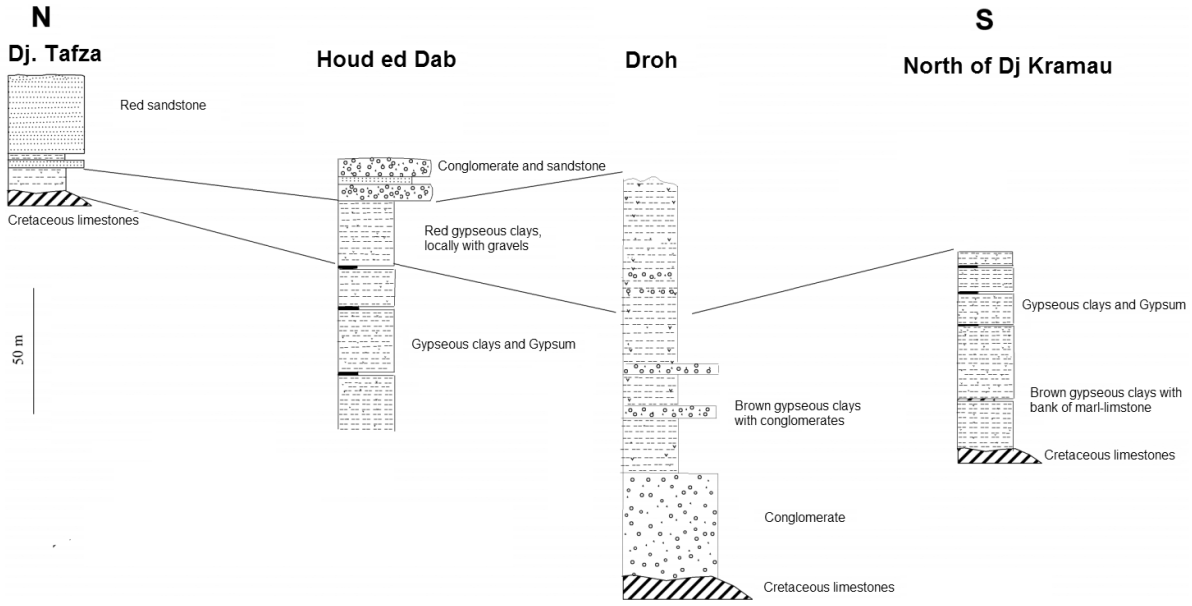

Fig. 4 - Log correlation between Djebel Kramau and Djebel Tafza, Droh Area (Chebbah, 2007).

Fig. 4 - Correlazione litologica tra Djebel Kramau e Djebel Tafza nell'area di Droh (Chebbah, 2007).

Hydrogeological setting

Hydrogeological studies (Chabour, 2008; Haouchine, 2010; Brinis, 2011; Abderrezzak, 2015) confirmed the presence of several heterogeneous aquifers hosted respectively in the Quaternary, Mio-Pliocene, Lower Eocene, Upper Senonian (Maastrichtian), and Albian formations. Three main aquifers have been identified in Biskra (Fig. 5): the Quaternary aquifer, the Complex Terminal (CT) aquifer and the Continental Intercalar.

The Quaternary aquifer of Biskra is constituted over 60 m by pebbles, dunes, sandy and stony alluvium (Sedrati, 2011).

The CT is identified in Upper Cretaceous and Tertiary layers including the Mio-Pliocene with sandy-clayed-sandstone, the evaporite Eocene, clays with gypsum, the upper Senonian with permeable formations, lower lagoon Cenomanian deposits with low permeability, carbonate and dolomitic Turonian. The Mio-Pliocene consists of an intercalation of discontinuous levels promoting communication between permeable formations. In the Eastern part, the pumped aquifer is constituted by Pliocene conglomerates; the center is occupied by the Miocene and Quaternary aquifer of Oued Biskra. Agricultural users pump in the Eocene limestone in the western limit where the neogenic filling is rather low.

The CT is subdivided into three aquifer levels:

– The first sandy aquifer with a limited depth (50 -100 m).
– The second Mio-Pliocene sandy aquifer is composed of sandstones, gravel, and sand with local clay lenses. The isopach map shows an aquifer thickness ranging from 60 to 420 m (Sedrati et al., 2008). Permeable thickness occurs irregularly, a decrease was observed from the East to the West with a large thickness of 420 m recorded near Biskra-Chetma. However, a reduced thickness was observed in the South-West. Currently, the aquifer is the most pumped (ANRH, 2008).
– The lower Eocene limestone aquifer is composed of cracked white limestone (Lower Eocene) and marl and dolomitic limestone (Upper Senonian); the top is composed of Mio-Pliocene sandy clay formations in the North and Eocene gypsum marls in the South (Sedrati, 2011). We note the presence of an aquitard from Middle Eocene represented by evaporite and marl deposits, a Maastrichtian-Campanian aquifer composed of limestone of Upper Cretaceous to Lower Eocene and hosting a karst aquifer with a total thickness ranging from 400 to 500 m; Santonian-Coniacian aquiclude with intercalation of evaporite deposits on 100 to 300 m of thickness, Turonian aquifer composed of limestone deposits in hydraulic communication with limestone aquifer and Cenomanian aquiclude (Ghiglieri et al., 2021). Indeed, the isopach map shows that limestone aquifer thickness varies from 50 m to 260 m. The thickening occurs in parallel with its deepening in Chetma between 50 to 170 m (Sedrati et al., 2008). However, we note the absence of the Upper Senonian aquifer in the North-East and a good synchronic correlation between the hydraulic heads and flexures.

Due to its deep dipping up to 750 m, Droh Syncline is not pumped in the North. However in the South-West, a complex aquifer composed of Lower Eocene limestone is pumped at 400 m of depth constituting the Droh pumping field. Nevertheless, high water salinity results from the dissolution of evaporative minerals (gypsum, anhydrite, and halite) unsaturated in halite, dry residue was measured at 5g/L and electrical conductivity between 1110 and 5940 µ.S/cm (Brinis, 2003; Brinis, 2011).

The Continental Intercalar in Biskra is identified in outcrops and at variable depths (1600–2500 m) and hosted in Lower Cretaceous formations (Aptian to Albian). The withdrawal rate is 39 hm^3/year (Burgeap, 1963; ANRH, 2008).

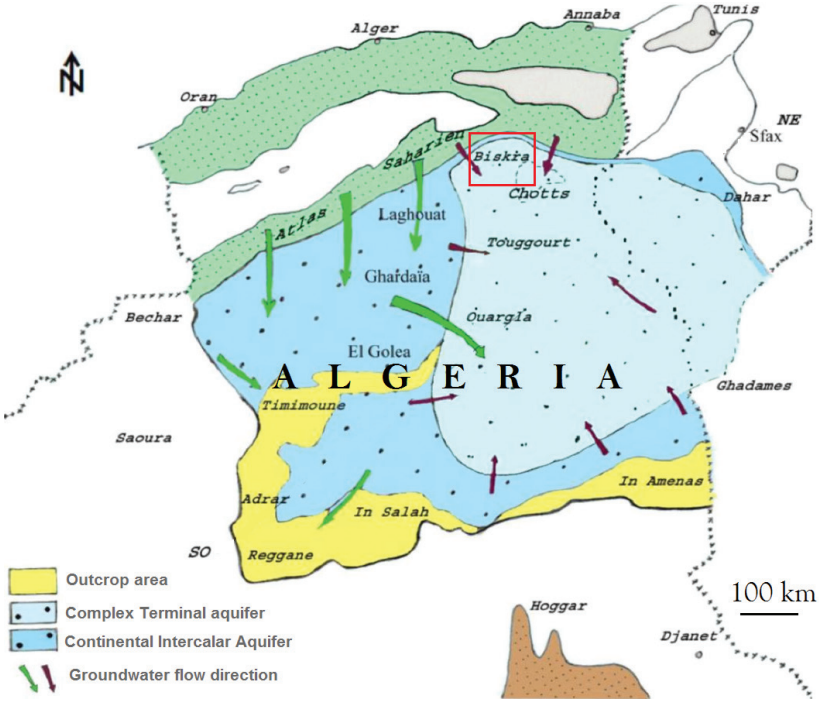

Fig. 5 - Hydrogeological map of the Complex Terminal and Continental Intercalar (UNESCO, 1972).

Fig. 5 - Carta idrogeologica degli acquiferi Complex Terminal e Continental Intercalar (UNESCO, 1972).

Geophysical investigation

A geophysical investigation was conducted in 2002 (ENAGEO, 2002). The aim was to estimate electrical resistivity, evaluate geometric characteristics and identify the geological and aquifer structures for a suitable implementation of a pumping device. Involving 109 vertical electrical soundings distributed over 13 profiles (Fig. 6), all profiles have a NW-SE orientation on which measurements were carried out with an equidistance of 1,000 m, except for profile H. Potentiometric recorder instrument and a GPS were used along with Schlumberger quadrupole. The length of the maximum emission line AB was fixed at 2000 m. The method consists in injecting a direct or alternating current between two injection electrodes A and B in the soil and measuring a potential difference generated by the passage of the current between two receiving electrodes M and N. Such VES were then interpreted using IPI2Win software 1D in order to calculate the final resistivity model. A semi-automatic iterative approach was used to refine the initial model for analyzing the resistivity data. The iteration calculation is continued until the difference between the observed and theoretical curves is reduced. The final model having the least error represents the layer parameters of the electrical sounding. Nevertheless, the software provides non-conforming distributions and uncertainties associated with the optimized model. As such, it was necessary to adjust the numerical optimization results with the lithological formations. The correlation was performed using six mechanical drillings (Fig. 7).

Results and discussion

Vertical Electrical Soundings (VES)

Several levels and thin pasts were identified. A topsoil ranging between 3 and 15 m in thickness and 10 to 343 Ωm corresponds to the Quaternary aquifer. It's composed of sand, ancient terraces formed by sandy and clayey deposits towards the south of Biskra, medium terraces composed of limestone and gypsum formations over 2 m and finally current terraces composed of dunes and alluvial sandy. The topsoil shows an accumulation of different soluble salts. It's followed by CT aquifer composed successively of a thick conductive deposit of Eocene marl limestone of 125 m and 87 Ωm and two resistant levels of 226.6 Ωm and 93 m and 776 Ωm over 15 m at C8. The Maastrichtian limestone aquifer with a dense network of diaclases was identified at 247 m of depth with an average resistivity of 200 Ωm. At D4, Maastrichtian aquifer was measured from 37 m of depth at 181 Ωm and covered by conductive cover of 12.5 Ωm. However at E1, it's appeared at 774 m of depth with 380 Ωm and was surmounted by thick conductive levels (10.7-61.1 Ωm) associated with clay. At H4, Maastrichtian massive limestone was investigated at 360 m of depth with 894 Ωm surmounted by a thick and conductive level (81 Ωm and 330 m).

Apparent iso-resistivity maps

A number of 62 measurements were used to create apparent iso-resistivity maps. At AB = 100 m (Fig. 8a), the reached depth was comprised from 12.5 according to Roy (1971) to 19 m according to Barker (1989). Indeed, it revealed the existence of a resistant anomaly in the Northeast of Biskra centred around C6, D6, and D7. It showed substantially high electrical resistivity (287-350 Ωm) corresponding to Mio-Pliocene sandstones and surmounted by a thin past of clay. In the East of Biskra, a second resistant and restricted anomaly appears divided over two main axes : one constituted under D2, F3, and H4, which is representative of the NE-SW direction and whose resistivity varies between 250 and 313

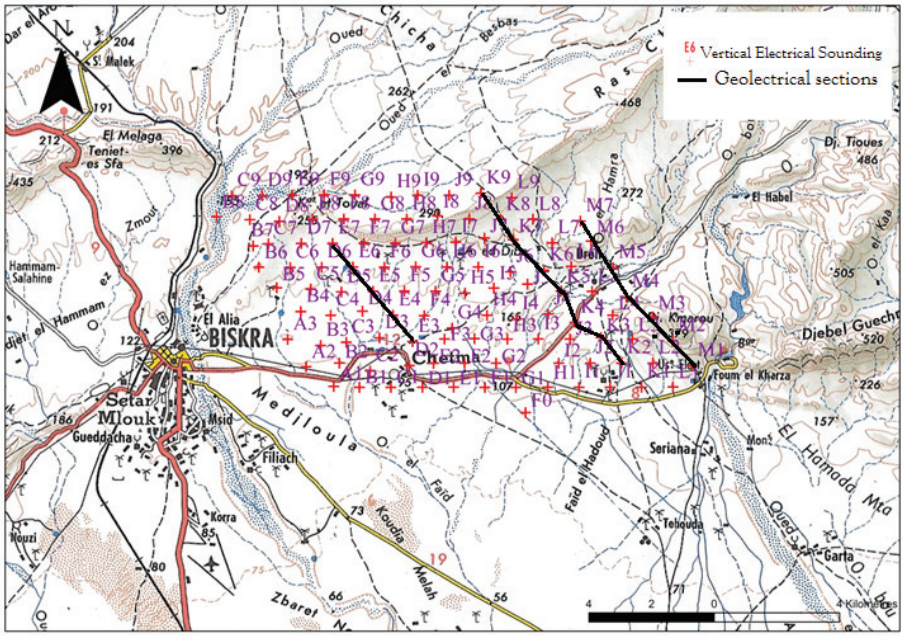

Fig. 6 - Location of the Vertical Electrical Soundings (VES) and profiles in Chetma-Biskra region.

Fig. 6 - Ubicazione dei sondaggi elettrici verticali (VES) e relativi profili nella regione Chetma-Biskra.

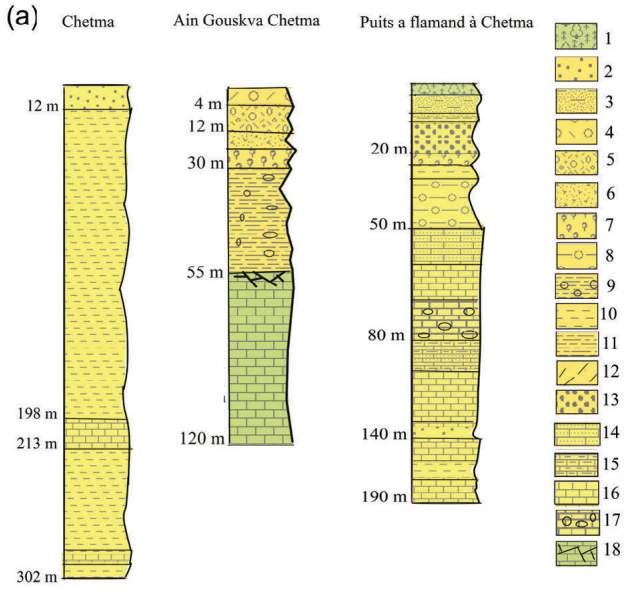

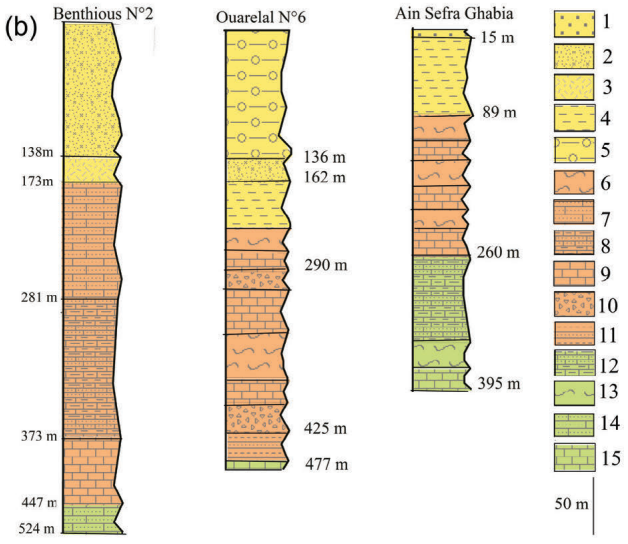

Fig. 7 - Lithological logs from boreholes localized close to the investigated site used in calibration.
(a): 1. topsoil, 2. sand (Mio-Pliocene), 3. sandy clay (Mio-Pliocene), 4. gravel and clay (Mio-Pliocene), 5. clay and fine gravel (Mio-Pliocene), 6. clay and rare pebbles (Mio-Pliocene), red clay and rare gravel (Mio-Pliocene), 7. puddingstone (Mio-Pliocene), 8. puddingstone and clay (Mio-Pliocene), 9. clay and rare gravel (Mio-Pliocene), 10. clay (Mio-Pliocene), 11. Compact clay (Mio-Pliocene), 12. clay shales (Mio-Pliocene), 13. sandstone (Mio-Pliocene), 14. limestone and clay (Maastrichtian), 15. limestone and marly (Maastrichtiano), 16. limestone (Maastrichtian), 17. grey and rare fissured limestone ; marly limestone ; grey and pink limestone ; white limestone ; limestone and marl ; soft and compact white and grey limestone (Maastrichtian), 18. coarse limestone (Maastrichtian)
(b): 1. sand (Mio-Pliocene), 2. sand and gravel (Mio-Pliocene), 3. conglomerate sandstone (Mio-Pliocene), 4. red clay (Mio-Pliocene), 5. clay gypsum (Mio-Pliocene), 6. marl (Eocene), 7. marly limestone (Eocene), 8. limestone gypsum conglomerate (Eocene), 9. Limestone (Eocene), 10. Dolomite (Eocene), 11. marly limestone and gypsum (Eocene), 12. marly limestone (Maastrichtian), 13. marl (Maastrichtian), 14. dolomite limestone (Maastrichtian), 15. Limestone (Maastrichtian)

Fig. 7 - Profili litologici dei pozzi ubicati nell'area investigata ed usati per la calibrazione
(a): 1. topsoil, 2. sabbia (Mio-Pliocene), 3. argilla sabbiosa (Mio-Pliocene), 4. ghiaia e argilla (Mio-Pliocene), 5. argilla e ghiaia fine (Mio-Pliocene), 6. argilla con rari ciottoli (Mio-Pliocene), argilla rossa con rara ghiaia (Mio-Pliocene), 7. conglomerato (Mio-Pliocene), 8. conglomerato e argilla (Mio-Pliocene) , 9. argilla e rara ghiaia (Mio-Pliocene), 10. argilla (Mio-Pliocene), 11. argilla compatta (Mio-Pliocene), 12. scisto argilloso (Mio-Pliocene), 13. arenaria (Mio-Pliocene), 14. Arenaria e argilla (Maastrichtiano), 15. calcare e marna (Maastrichtiano), 16. Calcare (Maastrichtiano), 17. calcare grigio raramente fessurato; calcare marnoso; calcare grigio e rosa; calcare bianco; calcare e marna; calcare tenero e compatto, bianco e grigio (Maastrichtiano), 18. calcare grossolano (Maastrichtiano)
(b): 1. sabbia (Mio-Pliocene), 2. sabbia e ghiaia (Mio-Pliocene), 3. arenaria (Mio-Pliocene), 4. argilla rossa (Mio-Pliocene), 5. gesso argilloso (Mio-Pliocene), 6. marna (Eocene), 7. calcare marnoso (Eocene), 8. calcare, gesso, conglomerato (Eocene), 9. calcare (Eocene), 10. dolomite (Eocene), 11. Calcare marnoso e gesso (Eocene), 12. calcare marnoso (Maastrichtiano), 13. marna (Maastrichtiano), 14. dolomite, calare (Maastrichtiano), 15. calcare (Maastrichtiano)

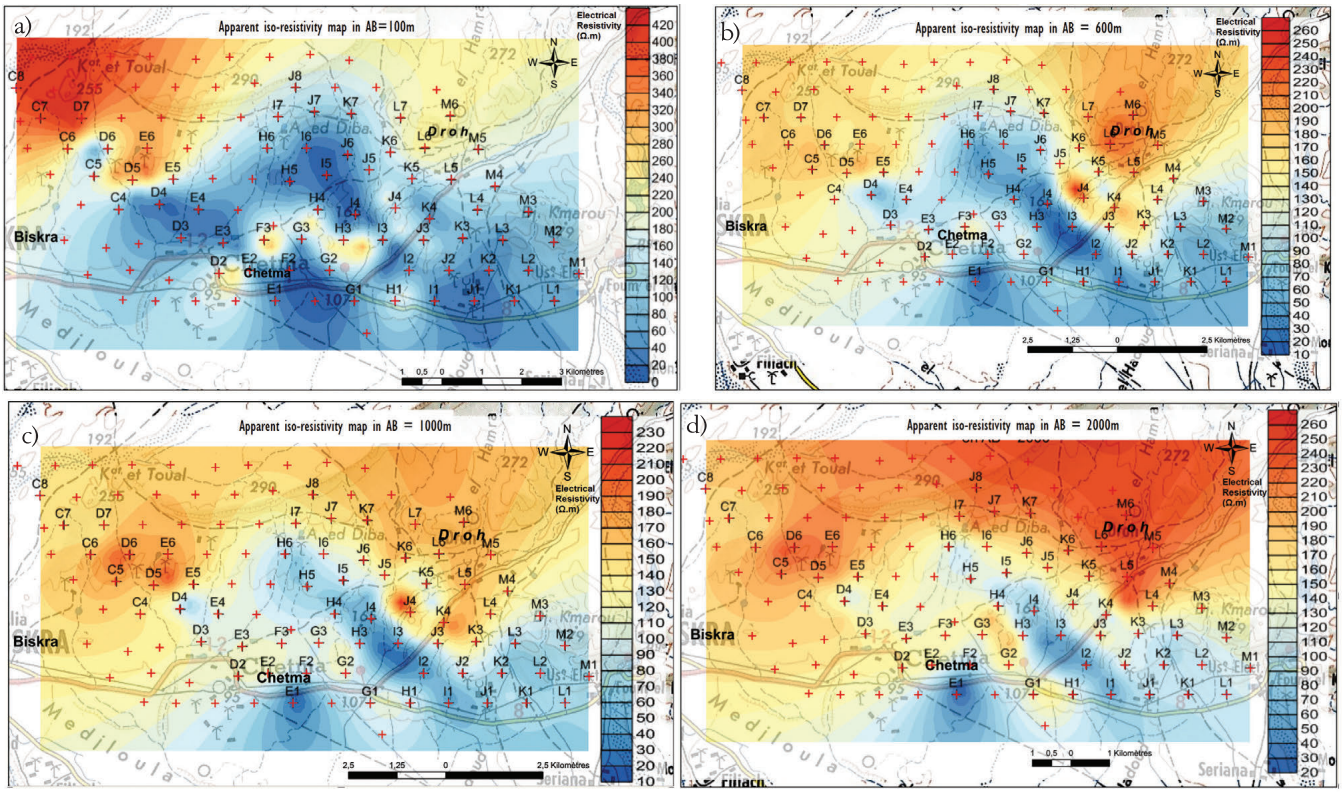

Fig. 8 - Apparent iso-resistivity maps in a) AB = 100 m, b) AB = 600 m, c) AB = 1000 m, d) AB = 2000 m.

Fig. 8 - Carte di resistività apparente a) AB = 100 m, b) AB = 600 m, c) AB = 1000 m, d) AB = 2000 m.

Ωm and the other consisting of I3, H3, and H4, represents the NW-SE direction with a resistivity average of 320 Ωm. Everywhere else, ranges represented in blue correspond to a conductive formation not exceeding 100 Ωm. According to Chetma's mechanical sounding (Fig. 5a) deep about 302 m, and composed of red clay with a limestone bank of 15 m of thickness, this filling was associated with the Mio-Pliocene red clays covered by 12 m of sand. With an AB = 600 m reaching a depth ranging from 75 to 114 m (Fig. 8b), two resistant anomalies were revealed. The first anomaly is located in the North-West with resistivities varying between 150 and 200 Ωm of Maastrichtian hard grey limestone. As this anomaly extends to the south, resistivities tend to decrease (120-140 Ωm). A second anomaly appears towards the East, resistivities vary between 130 and 230 Ωm representing a Maastrichtian hard grey limestone surmounted by Mio-Pliocene clay. However, a conductor corridor with NW-SE direction consisting of Mio-Pliocene red clays was identified between these two resistant ranges.

With an AB = 1,000 m reaching a depth from 125 to 190 m, two large resistant anomalies (<233 Ωm) were confirmed (Fig. 8c). The first one was located in the North-East of Biskra and centered around C8, C7, D7, C6, E6, and D6 with resistivity oscillating between 160 and 210 Ωm. This latter extends in the South. An alternation of hard grey limestone, red and black clay pasts, and Maastrichtian siliceous limestone were associated. The second anomaly was located in Droh with resistivity varying between 110 and 200 Ωm. Additionally, grey and white limestone and sometimes marl were attributed. Between the two resistant ranges, a conductor corridor of red clays was identified. A deeper structural form was confirmed consisting of two resistant anticlines separated by a conductive deposit syncline. The limestone anticline widens while the clay deposit syncline shrinks. Finally, the apparent iso-resistivity map in AB =2,000 m would reach deep levels between 250 and 380 m (Fig. 8d). In Droh, a wide range was characterized by high resistivities extending from C7 (237 Ωm), C6 (207 Ωm), D6 (217 Ωm) to M6 (225 Ωm), M5 (221 Ωm), M4 (249 Ωm). It was composed of limestone and marl with Maastrichtian gypsum intercalations. In-depth, the basement appears to be laterally continuous, consequentially an increasingly narrow conductive range occupies the syncline designed by the two anticlines. It was associated with a conductive deposit of red and black clays (< 100 Ωm).

Geoelectrical sections

The Geoelectrical section D in the NW-SE illustrates three contrasting levels(Fig. 9a). The first one is a thin topsoil (2-14 m) and conductive (55-78 Ωm) associated with Mio-Pliocene red clay, cover sand, and sandy-clayed-sandstone. Superimposing a thick (3-28 m) and more conductive level (10-25 Ωm) which is due to Eocene evaporate pasts, clays with gypsum and salt pasts. The third level is more resistant associated with limestone ranged from 134 to 232.5 Ωm. Geoelectrical section J (Fig. 9b) is represented by two main

levels, the first one represents a conductive filler composed of a succession of Mio-Plio-Quaternary fillers (46-120 Ωm) of sand, clay, and Quaternary alluvial materials, gypseous clay (4-10 Ωm) with thickness gathered between 15 and 33 m. The second one represents straightened resistant and fractured bars (200 to 500 Ωm) in the form of an anticline attributed to the Lower Eocene and Upper Senonian limestone (Maastrichtian and Campanian aquifers). Geoelectrical section L (Fig. 9c) illustrates a thin (2-4 m) and resistant level (114-262 Ωm) associated with gravel, sand, and clay of Mio-Plio-Quaternary, covering a thick (2-29 m) and conductive level (9-33 Ωm) attributed to Middle Eocene clay with frequent gypsum and salt pasts and finally a resistant level (147-409 Ωm) associated with limestone. The fractured and karstified limestone was recorded at 200 Ωm, however, the massive limestone was recorded at high resistivity (>500 Ωm).

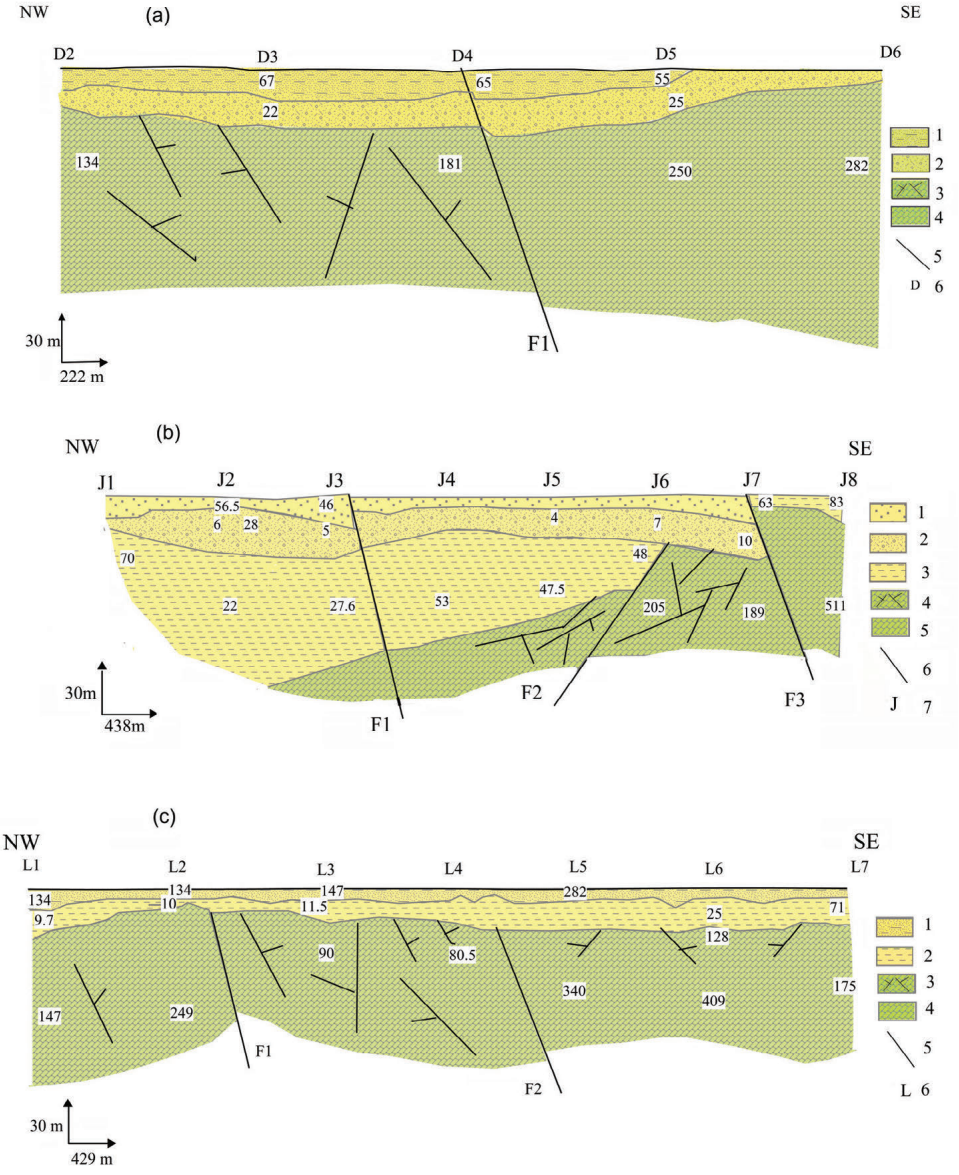

Fig. 9 - Geoelectrical sections along three profiles named D, J and L at Chetma-Biskra region
(a): 1. clays and sands from the Mio-Pliocene (Neogene), 2. salt and gypsum from the Mio-Pliocene and Eocene (Neogene), 3. limestone from Lower Eocene, upper Senonian and Maastrichtian (Paleogene-Upper Cretaceous), 4. fault, 5. vertical electrical sounding; (b): 1. sands from the Mio-Pliocene (Neogene), 2. salts and gyps from the Mio-Pliocene (Neogene), 3. clays from the Mio-Pliocene (Neogene), 4. limestone from Lower Eocene, Upper Senonian and Maastrichtian (Paleogene-Upper Cretaceous), 5. cracked limestone, 6. fault , 7. vertical electrical sounding and, (c): 1. gravel clays and sands from Mio-Pliocene (Neogene), 2. clays from Mio-Pliocene (Neogene) with gypsum and Salt, 3. limestone from Lower Eocene, Upper Senonian Maastrichtian limestone (Upper Cretaceous), 4. fault, 5. vertical electrical sounding.

Fig. 9 - Sezioni geoelettriche lungo tre profili chiamati D, J e L nella regione di Chetma-Biskra
(a): 1. Argille e sabbie del Mio-Pliocene (Neogene), 2. Sale e gesso del Mio-Pliocene e Eocene (Neogene), 3. Calcale dell'Eocene Inferiore, Senoniano Superiore e Maastrichtian (Paleogene-Cretaceo Superiore), 4. faglia, 5. sondaggio elettrico verticale; (b): 1. Sabbie del Mio-Pliocene (Neogene), 2. Sali e gessi del Mio-Pliocene (Neogene), 3. Argille del Mio-Pliocene (Neogene), 4. Calcari dell'Eocene Inferiore, Senoniano Superiore e Maastrichtian (Paleogene-Cretaceo Superiore), 5. Calcare fratturato, 6. faglia, 7. sondaggio elettrico verticale, (c): 1. Argille ghiaiose e sabbie del Mio-Pliocene (Neogene), 2. Argille del Mio-Pliocene (Neogene) con gesso e sale, 3. Calcale dell'Eocene Inferiore, Senoniano Superiore e Maastrichtiano (Cretaceo Superiore), 4. faglia, 5. sondaggio elettrico verticale.

Hydrogeological correlation

219 boreholes were collected, mostly are clustered in Droh and the South of Chetma and operated in the Mio-Pliocene aquifer, the most exploited aquifer (ANRH, 2008). Nevertheless, few boreholes are pumped in the Plio-Quaternary and the deeper aquifers (Lower Eocene, Senonian and Maastrichtian). Accordingly, only 29 boreholes (Fig. 10) were selected using a qualitative analysis in accordance to three criteria : boreholes located between 5-6° and 34-35°, boreholes pumping in the Mio-Pliocene aquifer and measured with a static level. The depth of boreholes increases from 60 to 220 m, water depth measured from surface ranges between 6 and 26 m, no artesian boreholes exist, pumping rate ranges between 1 to 33 L/s and mainly used for irrigation. A piezometric map was prepared using kriging interpolation. Measurement dates are not specified in ANRH Inventory. Caused by a complex structural context, a local hydrogeological deformations were observed with large piezometric fluctuations. Hydraulic heads, ranged from 30 m in the South to 297 m in the North-East, suggest high groundwater potentiality (Fig. 11). In the North-eastern of Droh, isopiezes appear more tighter and form a piezometric dome. Its considered as a recharge area with high piezometric levels measured at 280 m. However, isopiezes appear more spaced in the South and form a piezometric depression. Piezometric level decreases toward 50 m. The deeper boreholes are mainly located over the piezometric dome when piezometric levels are slightly higher. Piezometric levels appear rather low for medium depth boreholes located in the central part and shallow boreholes located in the South. Regional flow is characterized by a North-South direction. A North-South drainage water axis was identified as groundwater recharge flows. The piezometric dome was represented through the water divide line in the East of Droh. Three hydraulic gradient areas were identified:

- high hydraulic gradient area (20-50 ‰) in the North-East characterized by rapid flow velocity with good hydrodynamic properties due to the existence of a piezometric dome and depression. Indeed, pumping tests realized at borehole FC14-Droh provide a transmissivity of 49. 10^{-4} m²/s for the Lower Eocene-Maastrichtian limestone (ANRH, 2008);
- medium gradient area (10-14 ‰) in the central part;
- low gradient area (5 ‰) in the South reflecting a rather slow flow velocity.

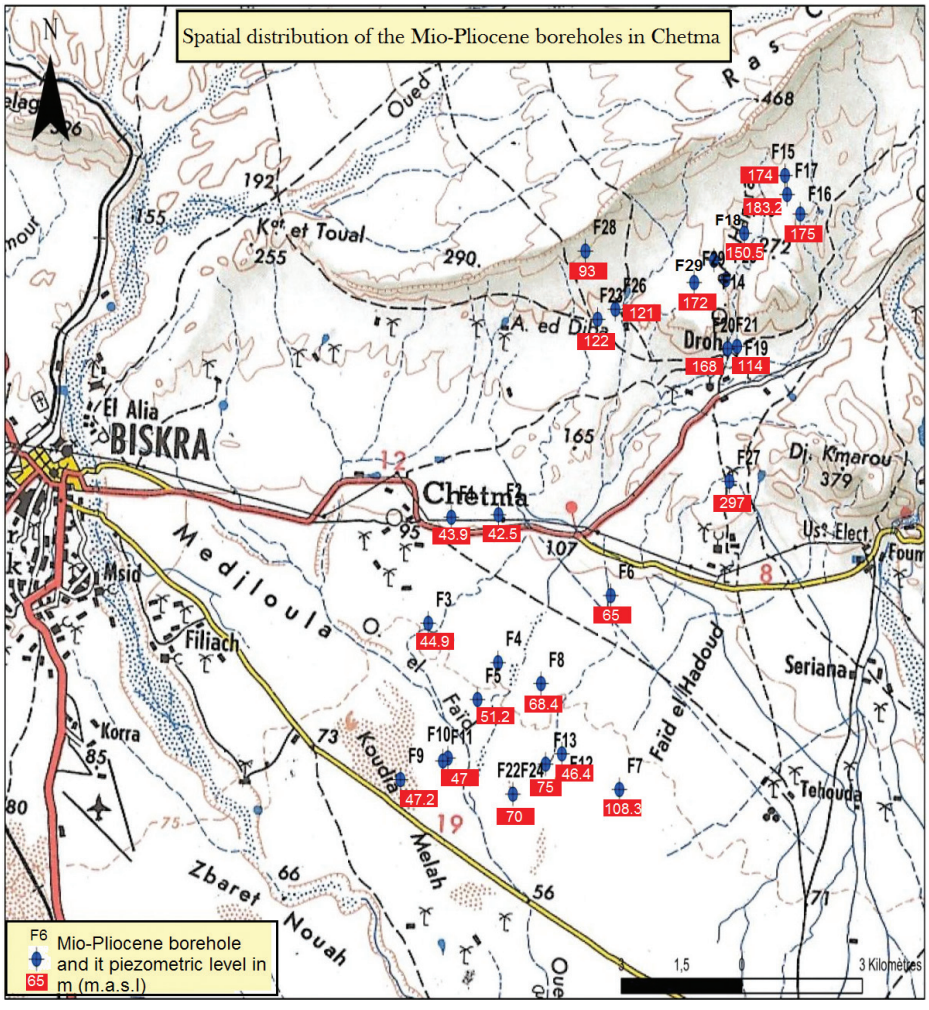

Fig. 10 - Spatial distribution map of the Mio-Pliocene boreholes in Chetma-Droh region.

Fig. 10 - Distribuzione spaziale dei pozzi captanti l'acquifero Mio-Pliocene nella regione Chetma-Droh.

According to piezometers located in the North-west and the South-west of Biskra, the piezometric level in the Mio-Pliocene and Lower Eocene aquifers which host the semi-deep aquifers is slightly decreased (ANRH, 2008; Drouiche et al., 2011; Arras et al., 2017). Due to the high pumped rate flows, these overexploited areas were specifically identified around piezometric depressions. Drawdown was measured at 10 m in the North and 34 m in the South.

The correlation between geophysical issues and ANRH piezometric investigations demonstrates that the piezometric dome overlays Droh anticline. Regional folds constitute structural highs and play an important role in recharging or dispersing surface water flows as confirmed by Ghiglieri et al. (2021). Due to their high piezometric level (290 m) and high hydraulic gradient (20-50 ‰), it was observed that deeper boreholes carried out in the Maastrichtian limestone at Droh provide significant groundwater yield with an average of 40 L/s. Note that the aquifer thickness increases in the North-East with 100 to 150 m (L4, L5, L6, M5, M6, O5) accordingly to resistivity increasing from 160 Ω.m at L4 to 215 Ω.m at P6. The higher the hydraulic gradient the greater the rate of groundwater flow through the aquifer. Moreover, boreholes at Droh are regularly pumped and none is abandoned. On the other hand, due to their low piezometric level and low hydraulic gradient, boreholes with medium and shallow depths were mostly abandoned. It was associated with a thick conductive syncline which consists of red clay and higher clay content and offers both low hydraulic conductivity and groundwater flow rates.

At Droh, deeper boreholes reaching the Maastrichtian limestone at 400 m and belonging to the Miocene, Eocene, and Paleocene levels were represented by high resistivities (Tab. 3). They capture a mixture of water giving high well yields ranged from 25 to 90 L/s. In fact, groundwater yields at 40 L/s are recorded in Maastrichtian limestone from deeper boreholes (>300 m), those ranged between 10 to 40 L/s are encountered at 300-400 m of depth. However, medium and shallow boreholes located in the South of Droh at the conductive syncline overlay a conductive area where the resistivity fall significantly. When boreholes were drilled at less depth (200-300 m), they pumped in the Mio-Pliocene aquifer composed of several clay and marl pasts which reduce their hydraulic conductivity and offer a low well yields (5 and 30 L/s). Boreholes drilled between 100 and 200 m of depth offer a pumping rate ranging from 1 to 20 L/s and finally boreholes drilled at less than 100 m of depth offer a limited well yields between 0.8 and 15 L/s. In addition, permeable thickness occurs irregularly and has a significant decrease from the East to the West with 420 m near Biskra and Chetma and 60 m in the West.

Considering that active boreholes were mainly aligned on the South-West to North-East as a dominant direction of regional faults and Atlas flexure, it improves the impact on the regional hydrogeology. The southern part nearby Biskra is mostly affected by tectonic lineaments, hence, the fault network facilitates hydraulic interconnection between different

Tab. 3 - Classification of water boreholes according to depth and flow rate in Biskra.

Tab. 3 - Classificazione dei pozzi per acqua di Biskra in base a profondità e portata di prelievo.

Depth (m)	Flowrate (L/s)
300-400	10 to 40
300-200	5 to 30
200-100	1 to 20*
< 100	0.8 to 15

*One borehole at 40 L/s

Aquifer formation	Flow rate (L/s)
Mio-Pliocene aquifer	1 to 20*
Maestrichtian aquifer	20 to 40

*One borehole at 40 L/s

aquifers. A mixing of groundwaters and hydrogeochemical quality (Abdennour et al., 2021; Ghiglieri et al., 2021; Semar et al., 2021) between saline and fresh groundwater resulted in a wide variability in resistivity. Local aquifers are separated by low permeable formations accelerating the inflow and outflow of groundwater where limestone was fissured. At Droh anticline, limestone consists of very cracked formation, thick about 200 to 350 m often producing high well yields. Together with Lower Eocene limestone form a complex aquifer pumped at 400 m of depth and constitute the Droh catchment field supplying Biskra. In this context, it's constitute a pattern that provides a potential groundwater productivity zones and the main path for groundwater flow. Indeed, antiform could strongly influence groundwater flow direction forcing the flow toward the informal axes and acting as storage areas allowing the accumulation of groundwater (Ghiglieri et al., 2021). However, synform geometries with high clay and marl content are not pumped by deeper boreholes. Nevertheless, in the axes of the syncline these are buried at high depths and boreholes having reached 750 m could offer interesting well yield for future pumping devices. To achieve the drinking water supply by 2030 projected about 35.14 hm^3/year and to ensure the groundwater sustainability in arid environment, we suggest to consider Droh as an excellent drilling site for future groundwater boreholes such as L4, L5 L6 et M4, M5, M6 with optimal depths comprised between 250 and 380 m. Thus, it would help local decision-makers to maximize water pumping without negative impact on the hydraulic head distribution.

Conclusion

Geophysical investigations combined to the geological and hydrogeological context of Chetma highlight the most relevant features and internal structures. High resistivities recorded in depth were associated with Maastrichtian marl limestone and limestone, while conductive deposit were attributed to red and black clays. A large agreement was assessed between electrical resistivity repartition and structural configuration. The latter was revealed on the shape of two anticlines. In depth, the basement appears to be continuous, consequentially an

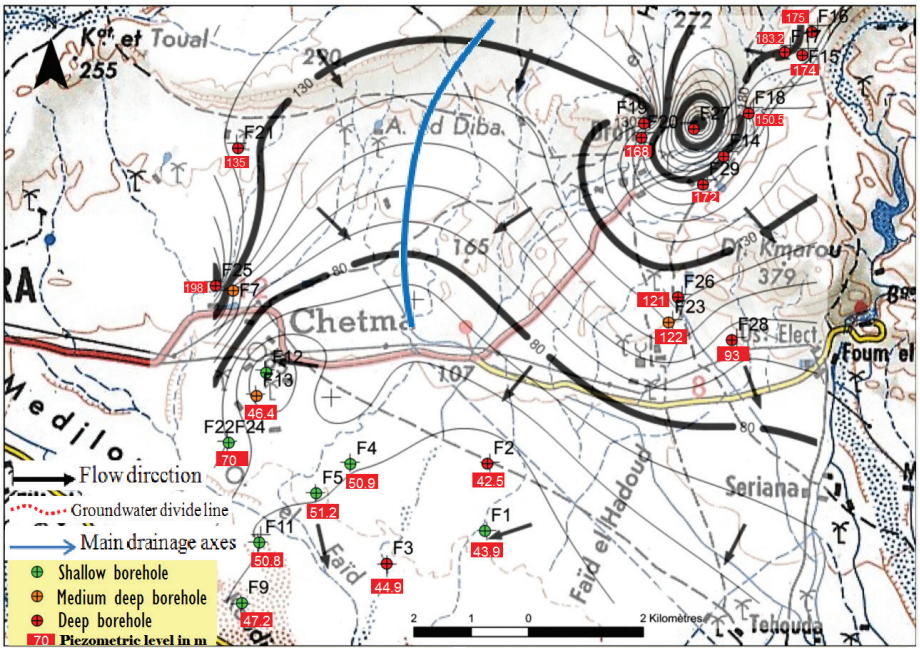

Fig. 11 - Piezometric map of the Mio-Pliocene aquifer.

Fig. 11 - Carta piezometrica dell'acquifero Mio-Pliocene.

increasingly narrow conductive range occupies the syncline. The hydrogeological study demonstrates the important role of groundwater in Biskra. The Mio-Pliocene aquifer is intensively pumped, however, due to high drawdown, more deep aquifers such as Complex Terminal aquifers are identified as hydrogeologically interesting. Droh piezometric dome superposes the anticline detected using geophysical prospecting. According to these results, it was suggested to local groundwater managers to consider the Droh area as an excellent drilling site for future groundwater exploitation.

Acknowledgement

The authors are immensely grateful to ENAGEO, SONATRACH and ANRH for their support. The authors are grateful to the support provided by the Algerian Direction of Scientific Research and Technological Development (DGRSDT).

Competing interest

The authors declare no competing interest.

Funding

The authors have not disclosed any funding.

Author contributions

All authors contributed to the study conception and design. Material preparation, data collection, GIS and geophysical process and result interpretation were completed by Farès KESSASRA, Nour-Houda Mezerreg, Djamel Eddine DEHIBI, Lamine DJARET, Asma BOUHCHICHA and Mohamed MESBAH. All authors read and approved the final manuscript.

Additional information

Supplementary information is available for this paper at https://doi.org/10.7343/as-2023-608

Reprint and permission information are available writing to acquesotterranee@anipapozzi.it

Publisher's note Associazione Acque Sotterranee remains neutral with regard to jurisdictional claims in published maps and institutional affiliations.

REFERENCES

Abdennour, M. A., Douaoui, A., Barrena, Pulido, M., Brada, A., Bennacer, A., Piccini, Ch. & Alfonso-Torren, A. (2021). Geochemical characterization of the salinity of irrigated soils in arid regions (Biskra, SE Algeria). Acta Geochimica (2021) 40(2):234–250 https://doi.org/10.1007/s11631-020-00426-2.

Abderrezzak, B. (2015). Hydrogéologie, vulnérabilité et modélisation de la nappe du Mio-Pliocène d'El Outaya, (Biskra, Sud-Est algérien) *"Hydrogeology, vulnerability and modelling of the Mio-Pliocene aquifer of El Outaya, (Biskra, South-East Algeria)"*. Thèse de Doctorat, Université Abou Bakr Belkaid Tlemcen, 179p

Albrecht, TR., Varady, RG., Zuniga-Teran, AA., Gerlak, AK. & Staddon, Ch. (2017). Governing a shared hidden resource: A review of governance mechanisms for transboundary groundwater security. Water Security, Volume 2, November 2017, Pages 43-56, https://doi.org/10.1016/j.wasec.2017.11.002.

ANRH (2008). Inventaire des forages et enquêtes sur les débits extraits de la wilaya de Biskra *"Inventory of boreholes and pumped flow rates of Biskra, Algérie"*.

Arras, C., Cau, PL., Buttau, C., Da Pelo, S., Carletti, A. & Ghiglieri, G. (2017). Groundwater numerical model of the Biskra inferoflux aquifer (NE Algeria). 3rd National Meeting on Hydrogeology Cagliari, IAH Italian Chapter University of Cagliari

Aidaoui, S. (1994). Ressources en eau et aménagement hydro-agricole dans la région de Biskra (Algérie) *"Water ressources and hydro-agricultural management in the Biskra region (Algeria)"*. Thèse Doct. d'état. Univ. Nancy II. France. 327 p.

Azffri, S.L., Faizan Ibrahim, M., Herwig Gödeke, S. (2022). Electrical resistivity tomography and induced polarization study for groundwater exploration in the agricultural development areas of Brunei Darussalam. Environmental Earth Sciences (2022) 81:233, https://doi.org/10.1007/s12665-022-10284-1

Ben Alayet, M., Ben Ghaffar, S., Zaghdoudi, S., Balti, H. & Gasmi, M. (2021). Contribution of electrical prospecting to the characterization of aquifers in the North Gabes-El Hamma region (Southern Tunisia). Journal of African Earth Sciences 178 (2021) 104159. https://doi.org/10.1016/j.jafrearsci.2021.104159.

Bersi, M. & Saibi, H. (2020). Groundwater potential zones identification using geoelectrical sounding and remote sensing in Wadi Touil plain, Northwestern Algeria. Journal of African Earth Sciences 172 (2020) 104014. https://doi.org/10.1016/j.jafrearsci.2020.104014.

Brinis, N. (2003) . Essai d'explication de la salinité des eaux de la nappe du Mio-pliocène d'El Outaya (Biskra) *"An attempt to explain the salinity of Mio-pliocene aquifer of El Outaya (Biskra)"*, mémoire de magister, Université d'Annaba, Algeria.

Brinis, N . (2011). Caractérisation de la salinité d'un complexe aquifère en zone aride-Cas de l'aquifère d'El Outaya, région nord-ouest de Biskra, Algérie *"Characterization of the salinity of a complex aquifer in an arid zone - Case of El Outaya aquifer, Northwest of Biskra, Algeria"*. Thèse de doctorat d'état. Université Mentouri, Algeria, 252p.

Bogardi, JJ. & Fekete , BM. (2021). Water: a Unique Phenomenon and Resource. J. J. Bogardi et al. (eds.), Handbook of Water Resources Management: Discourses, Concepts and Examples. https://doi.org/10.1007/978-3-030-60147-8_2.

Boucher, M., Favreau, G., Descloitres, M., Vouillamoz, JM., Massuel, S., Nazoumou, Y., Cappelaere, B. & Legchenko, A. (2009). Contribution of geophysical surveys to groundwater modelling of a porous aquifer in semiarid Niger: An overview, Comptes Rendus Geoscience 341 (2009) 800–809 803.

Burgeap (1963). Etude du Continental intercalaire saharien Study of the Saharan Continental intercalar, Technical report, DEMRH, Alger.

Busson, G. (1970). Le mésozoïque saharien : Essai de synthèse des donnés des sondages Algéro-Tunisiens *"The Saharan Mesozoic: An attempt to synthesize data from Algerian-Tunisian surveys"*. C.R.Z.A. Série Géol. N°11, Ed. CNRS, Paris. 810p.

Chabour, N. (2008). Hydrogéologie du domaine de transition entre l'Atlas saharien et la plate forme saharienne à l'Est de l'Algérie *"Hydrogeology of the transition domain between the Saharan Atlas and the Saharan platform in eastern of Algeria"*. PhD thesis, Université Constantine, Algeria. 176p.

Chabbah, M. (2007). Caractérisation sédimentologique et géochimique du Néogène, de part et d'autre de l'accident sud-atlasique, région de Biskra *"Sedimentological and geochemical characterization of the Neogene on bothsides of the South Atlatic accident, Biskra region"*. PhD thesis, Université Mentouri Constantine, Algeria. 417p.

Choudhury, K. & Saha, DK. (2004). Integrated Geophysical and Chemical Study of Saline Water Intrusion. Vol. 42, No. 5—GROUND WATER, 2004.

Drouiche, A., Harrat, N., Zahi, F., Boucham, N., Djabri, L. & Maftah, H. (2011). Highlight of piezometric fluctuations of groundwater through piezometrics network in the region of Biskra (Algeria). Journal of Materials and Environmental Sciences 2 (S1) (2011) 495-500, ISSN : 2028-2508CODEN

ENAGEO (2002). Etude géophysique par sondages électriques verticaux. Site Chetma Droh (W. Biskra) *"Geophysical study using vertical electrical soundings. Chetma Droh site (Biskra)"*. 11p.

ERESS (1972). Etude et gestion des ressources en eau du Sahara septentrional. Modèles mathématiques *"Study and management of water resources in the Northern Sahara. Mathematical models"*.

Famiglietti, J. (2014). The global groundwater crisis. Nature Climate Change 4, 945–948 (2014). https://doi.org/10.1038/nclimate2425.

Ghiglieri,G., Baba Sy.,MO., Yahyaoui, H., Ouessar , M., Ouldamara, A., Soler, IGi A., Arras, C., Barbieri, M., Belkheiri, O., Zaied, M.B., Buttau, C., Carletti, A., Da Pelo, S., Dodo, D., Funedda, A., Iocola, I., Meftah, E., Mokh, F., Nagaz, K., Melis, MT., Pittalis, D., Said, M., Sghaier, M., Torrentó, C., Virdis, S., Zahrouna, A. & Enne, G. (2014). Design of artificial aquifer recharge systems in dry regions of Maghreb (North Africa). Flowpath 2014 – National Meeting on Hydrogeology, 144-145, ISBN 978-88-907553-4-7 - https://doi.org/10.13140/2.1.1710.1764.

Ghiglieri, G., Buttau, C., ArrasC., Funedda, A., Soler, A., Barbieri, M., Carrey, R., Domènech, C., Torrentó, C., Otero. N., & Carletti, A. (2021). Using a multi-disciplinary approach to characterize groundwater systems in arid and semi-arid environments: The case of Biskra and Batna regions (NE Algeria). Science of the Total Environment 757 (2021) 143797. https://doi.org/10.1016/j.scitotenv.2020.143797.

Goldman, M. &, Neubauer, FM. (1994). Groundwater exploration using integrated geophysical techniques. Surveys in Geophysics 15: 331. https://doi.org/10.1007/BF00665814.

Gouskov, N. (1962). Notice explicative de la carte géologique au 1/200 000 Biskra *"Geological map note at 1/200,000 Biskra"*. Publ. Serv. Géol. Algérie.

Guendouz, A. & Michelot, JL. (2006). Chlorine-36 dating of deep groundwater from northern Sahara; Journal of Hydrology (2006) 328, 572– 580.

Guiraud, R. (1970). Sur la présence de décrochements dextres dans l'Atlas Saharien. Interprétation mégamétrique *"On the presence of dextral offsets in the Saharan Atlas. Megametric interpretation"*. C. Som. S.G.F, 8, pp. 316-318.

Guiraud, R. (1973) . Evolution post-Triasique de l'avant pays de la chaine alpine en Algérie d'aprés l'étude du bassin du Hodna et des régions voisines *"Post-triassic evolution of the Algerian front country of the Alpine chain based on the study of the Hodna basin and neighbouring regions"*. Thèse Sci. Univ. Nice, 270 p, 114 fig., 12 pl. h.t.

Guiraud, R. (1990). Evolution post-triasique de l'avant pays de la chaîne alpine en Algérie d'après l'étude du bassin du Hodna et des régions voisines *"Post-triassic evolution of the Algerian front country of the Alpine chain based on the study of the Hodna basin and neighbouring regions"*. Pub.ONG, Alger. 259p.

Haouchine, A. (2010). Hydrogéologie en zone semi-aride et aride: Région de Biskra *"Hydrogeology of a semi-arid and arid zone: Biskra region"*. Thèse de doctorat d'état en Hydrogéologie de l'USTHB. 155p.

Laffite, R. (1939). Etude géologique de l'Aurès *"Geological study of the Aures"*. Bull. Serv. Carte géol. Algérie, 2èmesérie, Stratigr. Descript. Région. N°15, 451p.

Lehner, B., Liermann, CR., Revenga, C.,Vörösmarty, C., Fekete, B., Crouzet, P., Döll, P., Endejan, M., Frenken, K., Magome, J., Nilsson, C., Robertson, JC., Rödel, R., Sindorf, N. & Wisser, D. (2011). High-resolution mapping of the world's reservoirs and dams for sustainable river-flow management. Frontiers in Ecology and the Environment 9(9):494–502.

Molle F. & Closas, A. (2017). Groundwater Governance: A Synthesis Groundwater Governance in the Arab World - Report no. 6 April 2017, 186p.

PNE (2010). Réalisation de l'étude d'actualisation du Plan National de l'Eau *"(PNE) to Study to update the National Water Plan"*. Rapport final.

Ouali S., Khellaf A. & Baddari K. (2007). Etude des ressources géothermiques du sud algérien *"Study of the geothermal resources of the Algerian South"*, Revue des Energies Renouvelables Vol. 10 N°3 (2007) 407 – 414

Remini B., Merzoug H, Rais M.A. (2018). Le barrage de Foum el Gherza (Algérie) : quand l'eau coule dans le massif karstique *"The Foum el Gherza dam (Algeria): when water flows in the karst massif"*, Larhyss Journal, 36 (2018), 179-198

Sedrati, N., Bouchahm, N., Chaib, W., Rezeg, A., Slimani, R., Benaouda, L. & Djabri, L. (2008). Apports de la géophysique pour la détermination de l'extension des aquifères de la région de Biskra *"Geophysical inputs to identify the extension of aquifers of Biskra region"*. Journal Algérien des Régions Arides, N° 07 - 2008, Algeria.

Sedrati, N. (2011). Origine et caractéristiques physico-chimique des eaux de la willaya de Biskra sud-est algérien *"Origin and physico-chemical characteristics of the waters of Biskra in the South-eastern of Algeria"*, thèse de doctorat, Université d'Annaba.

Semar, A., Bachir, H. & Bourafai, S. (2021). Hydrochemical characteristics of aquifers and their predicted impact on soil properties in Biskra region, Algeria. Egyptian Journal of Agricultural Research, (2021) (2),204-219. 10.21608/ejar.2021.56750.1068.

Wada, Y., van Beek, LPH., van Kempen, CHM., Reckman, JWTM., Vasak, S. & Bierkens, MFP. (2010). Global depletion of groundwater resources, Geophysical Research Letters, VOL. 37, L20402, https://doi.org/10.1029/2010GL044571, 2010.

UNESCO (1972). Etude des Ressources en Eau du Sahara Septentrional *"Water Resource Study in the Northern Sahara"*, UNESCO, Paris.